International Journal of Thermal Sciences 48 (2009) 1552–1563

Contents lists available at ScienceDirect

International Journal of Thermal Sciences

www.elsevier.com/locate/ijts

Heat transfer to power-law dilatant fluids in a channel with a built-in square cylinder

Amit Kumar Dhiman *

Department of Chemical Engineering, Indian Institute of Technology Roorkee, 247 667, India

ARTICLE INFO

Article history:
Received 17 April 2008
Received in revised form 17 December 2008
Accepted 17 December 2008
Available online 10 March 2009

Keywords:
Square cylinder
Dilatant fluids
Nusselt number
Prandtl number
Blockage
Constant temperature condition
Uniform heat flux condition

ABSTRACT

In this study, heat transfer to power-law dilatant fluids from a long square cylinder (heated) confined in a channel in the steady flow regime is investigated. The effects of Reynolds number, Prandtl number and flow behavior index on the heat transfer characteristics of a cylinder is examined for the range of conditions $1 \leqslant Re \leqslant 45$, $1 \leqslant n \leqslant 2.0$ and $1 \leqslant Pr \leqslant 100$ (the maximum Peclet number being 4000) for a fixed blockage ratio, $\beta = 1/8$. The variation of the local Nusselt number on the individual surfaces of the square obstacle for the constant wall temperature (CWT) and uniform heat flux (UHF) boundary conditions prescribed on the surface of the square obstacle are presented. Likewise, the representative isotherm plots for the two classical thermal boundary conditions are shown. The average Nusselt number and the heat transfer factor (j_h) have also been calculated. Irrespective of the value of the flow behavior index, the value of the local Nusselt number at each corner of the square cylinder increases with an increase in the Reynolds and/or Prandtl number. The average Nusselt number increases monotonically with an increase in the Reynolds and/or the Prandtl number. Finally, simple heat transfer correlations have been provided for the range of conditions covered here.

1. Introduction

The fluid flow across cylinders (square or circular cross-section) exhibits a rich variety of flow regimes depending upon the value of the Reynolds number, power-law index and the flow domain (confined or unconfined) [1–15]. Most multiphase mixtures, i.e., foams, suspensions, emulsions, etc. and high molecular weight polymeric systems, i.e., solutions, melts, blends, etc. exhibit shear-thinning (pseudo-plastic fluids, $n < 1$) and/or shear-thickening (dilatant fluids, $n > 1$) behaviors under appropriate flow conditions and the simple non-Newtonian power-law model is able to describe satisfactorily both the shear-thinning and shear-thickening behaviors over moderate ranges of shear rates [16–18]. In spite of such a wide occurrence of power-law fluids, very little is known about the heat transfer characteristics of a heated cylinder of square or circular cross-section confined in a channel.

Indeed, there are only a few numerical heat transfer studies from the circular cylinder to power-law fluids in both confined and unconfined flow configurations [7,14,15]. Soares et al. [7] investigated the forced convection heat transfer from an unconfined circular cylinder for the range $5 \leqslant Re \leqslant 40$, $1 \leqslant Pr \leqslant 100$ and $0.5 \leqslant n \leqslant 1.4$. They used the stream-function/vorticity formulation to solve the governing momentum and thermal energy equations. They reported that the effect of power-law index on the local Nusselt number was less pronounced for the constant temperature condition than that for the uniform heat flux condition. The average Nusselt number was found to be a decreasing function of power-law index; however, for lower value of the Peclet number such dependence was found to be less pronounced. Along the same lines, Bharti et al. [14] investigated the heat transfer from an unbounded circular cylinder to power-law fluids for $0.6 \leqslant n \leqslant 2.0$, thereby covering the weak shear-thinning and strong shear-thickening fluids. The numerical investigations have been carried out by using finite volume method (FVM) for $1 \leqslant Pr \leqslant 1000$, but for the same range of Reynolds number as used by Soares et al. [7]. The pseudo-plastic fluids show higher heat transfer than that for Newtonian ($n = 1$) and dilatant fluids. Simple heat transfer correlations have also been established based on the numerical results. As far as channel confined circular object case is concerned, there is only one heat transfer study due to Bharti et al. [15] in the steady cross-flow regime. They investigated the effect of two blockage ratios (1/4 and 5/8) on the heat transfer characteristics of a circular cylinder for the range $1 \leqslant Re \leqslant 40$, $1 \leqslant Pr \leqslant 100$ and $0.2 \leqslant n \leqslant 1.8$ by using the commercial CFD package Fluent. They found the enhancement in the rate of heat transfer with the increasing degree of shear-thinning behavior; however, an opposite trend was observed in dilatant fluids for a fixed value of the blockage ratio. Aside from these studies, there have been numerous analyses based on the usual boundary layer approximation [9] and most

* Tel.: +91 1332 285890 (office), +91 9410329605 (mobile).
E-mail address: amitdfch@iitr.ernet.in.

1290-0729/$ – see front matter © 2008 Published by Elsevier Masson SAS.
doi:10.1016/j.ijthermalsci.2008.12.013

Nomenclature

b	side of a square cylinder ..... m
c_p	specific heat of the fluid ..... $J\,kg^{-1}\,K^{-1}$
h	local heat transfer coefficient ..... $W\,m^{-2}\,K^{-1}$
$\bar{h}$	average heat transfer coefficient ..... $W\,m^{-2}\,K^{-1}$
j_h	Colburn factor for heat transfer ($= Nu/(RePr^{1/3})$)
k	thermal conductivity of the fluid ..... $W\,m^{-1}\,K^{-1}$
L_1	length of the computational domain ..... m
L_2	height of the computational domain ..... m
m	power-law consistency index ..... $Pa\,s^n$
N_i	number of grid points in the x-direction
N_j	number of grid points in the y-direction
n	power-law index
n_s	normal direction to the surface of the cylinder
Nu	average Nusselt number ($= \bar{h}b/k$)
Nu_L	local Nusselt number ($= hb/k$)
p	pressure ($= p'/(\rho U_{max}^2)$)
Pe	Peclet number ($= RePr$)
Pr	Prandtl number ($= (mc_p/k)(U_{max}/b)^{n-1}$)
q_w	constant heat flux on the surface of the cylinder ..... $W\,m^{-2}$
Re	Reynolds number ($= \rho U_{max}^{2-n} b^n/m$)
T	temperature ($= (T' - T_\infty)/(T'_w - T_\infty)$ or $(T' - T_\infty)/(q_w b/k)$)
T_∞	temperature of the fluid at the inlet ..... K
T'_w	constant wall temperature at the surface of the cylinder ..... K
u	component of the velocity in the x-direction ($= u'/U_{max}$)
U_{max}	maximum velocity of the fluid at the inlet ..... $m\,s^{-1}$
v	component of the velocity in the y-direction ($= v'/U_{max}$)
x	stream-wise coordinate ($= x'/b$)
X_d	downstream face distance of the cylinder from the outlet
X_u	upstream face distance of the cylinder from the inlet
y	transverse coordinate ($= y'/b$)

Greek symbols

β	blockage ratio ($= b/L_2$)
δ	size of the control volume clustered around the cylinder ..... m
Δ	size of the control volume far away from the cylinder ..... m
ε	component of the rate of deformation tensor ($= \varepsilon'/(U_{max}/b)$)
η	power-law viscosity ($= \eta'/\eta_0$)
η_0	reference viscosity ($= m(U_{max}/b)^{n-1}$) ..... Pa s
I_2	second invariant of the rate of deformation tensor ($= I'_2/(U_{max}/b)^2$)
ρ	density of the fluid ..... $kg\,m^{-3}$
τ	extra stress component ($= \tau'/(\eta_0 U_{max}/b)$)

Subscripts

f, t, r	front, top and rear faces of the square cylinder, respectively
i	index used in the x-direction
j	index used in the y-direction
N	Newtonian
w	surface of the cylinder
∞	inlet condition

Superscript

$'$	dimensional variable

of these along with the scant experimental results have been reviewed in [16].

Similarly, there are only three previous numerical studies dealing with the heat transfer from a square obstacle to power-law fluids in the steady cross-flow regime [2,3,8]. Gupta et al. [2] examined the heat transfer from the confined cylinder to power-law liquids for $5 \leqslant Re \leqslant 40$, $0.5 \leqslant n \leqslant 1.4$ and $1 \leqslant Pr \leqslant 10$ ($5 \leqslant Pe \leqslant 400$) for both CWT and UHF conditions for a fixed blockage ratio of 1/8. They implemented the finite difference method (FDM) on a uniform staggered grid arrangement without any clustering around the cylinder and near the channel walls. Subsequently, Paliwal et al. [3] studied the heat transfer characteristics of an unconfined square obstacle over the identical ranges of the Reynolds number, Prandtl number and the flow behavior index as covered by Gupta et al. [2]. In gross, shear-thinning fluid behavior seems to facilitate heat transfer whereas shear-thickening behavior impedes it irrespective of whether the cylinder is confined or unconfined. In yet another similar study, Nitin and Chhabra [8] extended the work of Gupta et al. [2] for the heat transfer to power-law liquids from a cylinder of rectangular cross-section for the same range of conditions. Interestingly, it is worthwhile to point out here that in all these studies [2,3,8], a relatively coarse and uniform mesh was used having only about 10 cells on the each side of the cylinder. Therefore, these preliminary results are probably not very accurate, as confirmed by subsequent more accurate and detailed studies [12,19–24]. Recently, the effects of power-law index on the flow characteristics across the square cylinder have been studied for three values of the blockage ratio (1/8, 1/6 and 1/4) in [19]. In another recent study, Dhiman et al. [25] have investigated the mixed convection to power-law fluids from an isolated square cylinder in an unconfined flow configuration. Mixed convection effects have also been investigated in the channel confined steady flow regime in [26]. Therefore, it can be summarized here that very limited numerical results are available in the literature on the cross-flow of non-Newtonian dilatant fluids past a confined square cylinder. Thus, the objective of this work is to study the effects of Reynolds number and Prandtl number on the heat transfer across a confined long cylinder with square cross-section for dilatant fluids in the steady regime. Further, owing to high viscosity levels of many substances of multi phase nature and/or of high molecular weight (e.g., pulp and paper suspensions, polymer melts and biological process engineering applications, etc.), this study includes the results for power-law index up to 2.

2. Problem formulation

Two-dimensional, steady and incompressible fluid flow across a square cylinder confined in a channel is studied here, as shown in Fig. 1. The cylinder of side b is exposed to a parabolic velocity profile with maximum velocity, U_{max} and uniform temperature, T_∞ at the inlet. The non-dimensional distance from the inlet plane to the front surface of the cylinder is X_u/b, and the distance between the rear surface of the cylinder and the exit plane is X_d/b. The total non-dimensional length of the computational domain is L_1/b in the axial direction. The non-dimensional height of the computational domain is L_2/b in the lateral direction.

The continuity, x- and y-components (assuming negligible buoyancy effects) of Cauchy's equations [19] and of the energy

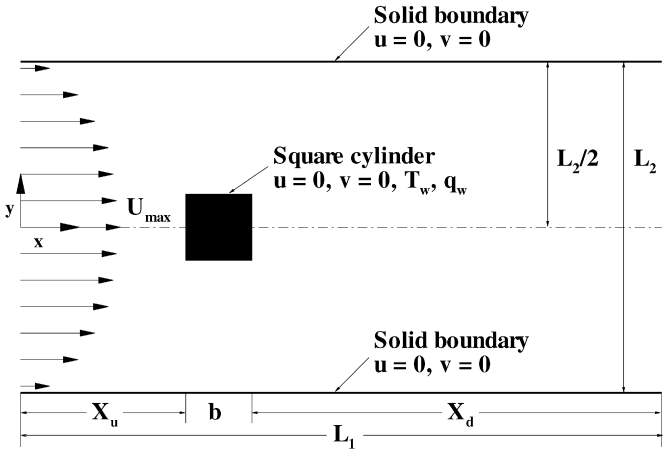

Fig. 1. Schematics of the flow around a confined square cylinder.

equation (assuming negligible viscous dissipation and constant thermo-physical properties) [23] in their dimensionless forms can be expressed as

Continuity equation:

$$\frac{\partial u}{\partial x}+\frac{\partial v}{\partial y}=0 \tag{1}$$

x-Momentum equation:

$$\frac{\partial u}{\partial t}+\frac{\partial (uu)}{\partial x}+\frac{\partial (vu)}{\partial y} = -\frac{\partial p}{\partial x}+\frac{\eta}{Re}\left(\frac{\partial^2 u}{\partial x^2}+\frac{\partial^2 u}{\partial y^2}\right)+\frac{2}{Re}\left(\varepsilon_{xx}\frac{\partial \eta}{\partial x}+\varepsilon_{yx}\frac{\partial \eta}{\partial y}\right) \tag{2}$$

y-Momentum equation:

$$\frac{\partial v}{\partial t}+\frac{\partial (uv)}{\partial x}+\frac{\partial (vv)}{\partial y} = -\frac{\partial p}{\partial y}+\frac{\eta}{Re}\left(\frac{\partial^2 v}{\partial x^2}+\frac{\partial^2 v}{\partial y^2}\right)+\frac{2}{Re}\left(\varepsilon_{yy}\frac{\partial \eta}{\partial y}+\varepsilon_{xy}\frac{\partial \eta}{\partial x}\right) \tag{3}$$

where $\varepsilon_{xx}=\partial u/\partial x$, $\varepsilon_{yy}=\partial v/\partial y$ and $\varepsilon_{xy}=\varepsilon_{yx}=1/2[\partial u/\partial y+\partial v/\partial x]$.

Energy equation:

$$\frac{\partial T}{\partial t}+\frac{\partial (uT)}{\partial x}+\frac{\partial (vT)}{\partial y}=\frac{1}{Pe}\left(\frac{\partial^2 T}{\partial x^2}+\frac{\partial^2 T}{\partial y^2}\right) \tag{4}$$

The power-law fluid behavior may be presented by

$$\tau_{ij}=2\eta\varepsilon_{ij}$$

and the apparent viscosity, η is given by

$$\eta=(I_2/2)^{(n-1)/2}$$

where $I_2/2=2(\partial u/\partial x)^2+2(\partial v/\partial y)^2+(\partial u/\partial y+\partial v/\partial x)^2$.

The boundary conditions for the momentum and energy equations in their dimensionless forms can be written as (Fig. 1).

Inlet boundary:

$$u=1-(2\beta y)^{(n+1)/n}, \qquad v=0,\ T=0,$$

where

$$\beta=b/L_2 \quad \text{and} \quad 0\leqslant y\leqslant L_2/2b$$

Upper boundary:

$$u=0, \qquad v=0, \qquad \partial T/\partial y=0$$

Square obstacle:

$$u=0, \qquad v=0, \qquad T=1 \text{ (CWT)} \quad \text{or}$$

$$\partial T/\partial n_s=-1 \text{ (UHF)}$$

Exit boundary:

$$\partial\phi/\partial x=0,$$

where ϕ is the dependent variable, u or v or T.

Plane of symmetry (i.e., at $y=0$):

$$\partial u/\partial y=0, \qquad v=0, \qquad \partial T/\partial y=0$$

Eqs. (1) to (4) along with the above-noted boundary conditions have been solved to obtain the local and average Nusselt numbers and the derived variables like stream function, etc. In this study, the local Nusselt number is defined as $-\partial T/\partial n_s$ and $1/T_w$ for the constant temperature and constant heat flux boundary conditions, respectively. The average Nusselt number for each surface of the square cylinder is obtained by averaging the local Nusselt number over the cylinder surfaces. The overall average Nusselt number is obtained by further averaging these values for each surface of the cylinder.

3. Numerical details

The computational grid structure consists of five separate zones with both uniform and non-uniform grid distributions having a close clustering of grid points in the regions of large gradients and the coarser grids in the regions of small gradients [19–21]. The grid distribution is uniform with a constant cell size, $\Delta=0.25b$, in an outer region that extends beyond 4 units from the cylinder. A much smaller grid size, δ, is clustered in an inner region around the cylinder to a distance of $1.5b$ to adequately capture the wake dynamics and steep temperature gradients close to the cylinder. The hyperbolic tangent function has been used for stretching the cell sizes between the limits of Δ and δ in x-direction [27]. Similarly, a fine grid of size, δ, is also clustered near the upper and lower bounding walls of the channel to resolve adequately the wake-wall interactions. An algebraic expression has been used for generating the grid points in the region $0.25b$ away from the cylinder and the channel walls in the y-direction [28].

The semi-explicit finite volume method on a non-staggered grid has been used to solve the unsteady governing equations [29]. Here, the momentum equations are discretized in an explicit manner while the pressure gradient terms are treated implicitly. However, the convective terms are discretized using the QUICK scheme as opposed to the central difference scheme (CDS) while the diffusive terms are discretized using CDS [19–21,30]. In order to discretize the non-Newtonian terms, CDS has been used [19].

The velocity fields obtained by solving the momentum equations from our recent study [19] are used as input to the energy equation. The explicit scheme has been used for the solution of the energy equation to obtain the temperature field over the range of values of $Re=1$–45, $Pr=1$–100 ($Pe\leqslant 4000$) and $1\leqslant n\leqslant 2.0$. The convective term is again discretized using the QUICK scheme while the diffusive term is discretized using CDS [23].

3.1. Choice of numerical parameters

The detailed study on the choice of numerical parameters for the flow of Newtonian fluids ($n=1$) across a square cylinder confined in a channel has been reported for $\beta=1/8$ in [21]. However, the non-Newtonian flow parameter study at various values of the power-law index for $\beta=1/4$ is well documented in [19].

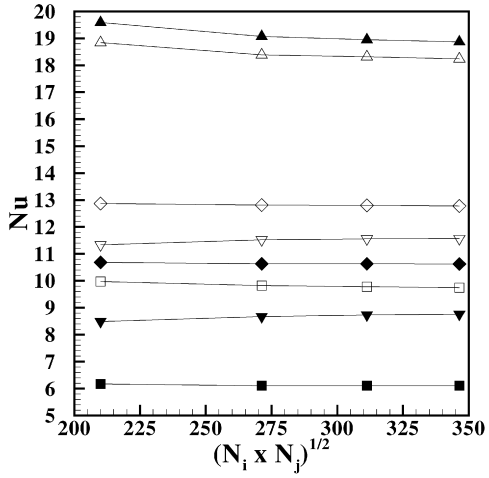

Fig. 2. Grid independence study for $Re = 45$ and $Pr = 50$ at $n = 1.5$. Filled and open symbols correspond to CWT and UHF conditions, respectively. The symbols ▲, ▼, ■ and ◆ represent the front surface, top surface, rear surface and average Nusselt numbers, respectively.

In the present study, some further exploration has also been carried out to examine the role of power-law rheology on the choice of these parameters for $\beta = 1/8$.

For the grid resolution study, four non-uniform orthogonal grids, $N_i \times N_j$ (225×196, 283×260, 323×300, 353×340 with 48, 80, 100, 120 cells on the each side of the cylinder, respectively) have been used for the maximum value of the Prandtl number of 50 for the Reynolds number of 45 at the power-law index of 1.5, as shown in Fig. 2. The relative changes in the values of the front surface average Nusselt number are found to be about 3.82%, 1.07%, 0.43% for 225×196, 283×260, 323×300 as compared to the value of the front surface average Nusselt number for the grid size of 353×340 for both the temperature conditions. However, the corresponding changes in the value of the average Nusselt are found to be about 0.72%, 0.26%, 0.18% for 225×196, 283×260, 323×300 as compared to the value of the average Nusselt number for the grid size of 353×340. In addition, limited grid independence study is also carried out for two grids (225×196 and 323×300 with 48 and 100 cells on the side of the cylinder, respectively) for the Prandtl number of 50, Reynolds number of 45 and the power-law index of 2.0. The differences between the two values of the front surface average Nusselt number and the overall average Nusselt

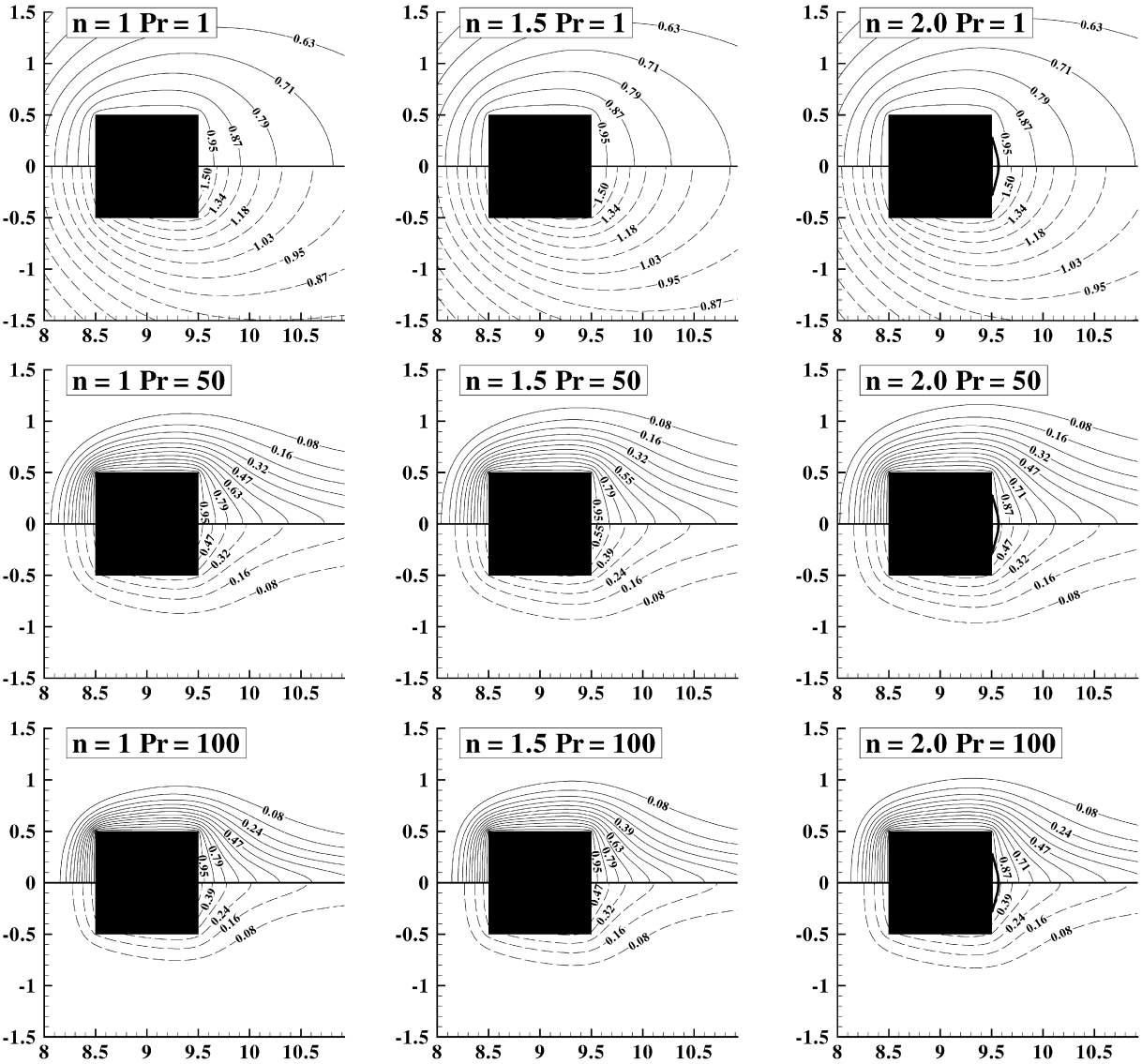

Fig. 3. Isotherms (upper and lower halves present the results for CWT and UHF cases, respectively) for $Re = 1$ and for $n = 1$, 1.5, 2.0 at different Prandtl numbers. The streamline representing the closed near wake at $n = 2.0$ is shown by a thick line.

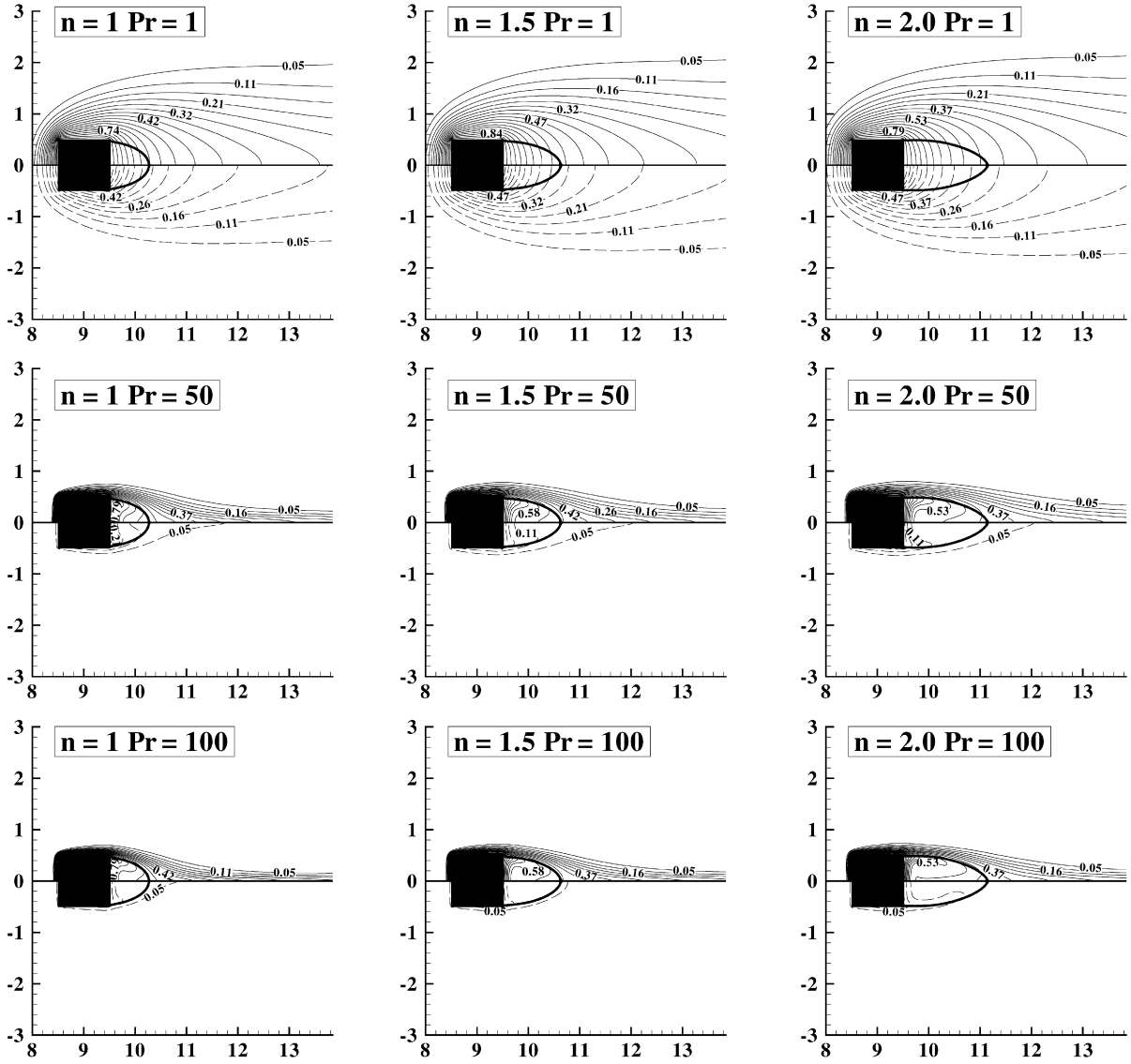

Fig. 4. Isotherms (upper and lower halves present the results for CWT and UHF cases, respectively) for $Re = 15$ and for $n = 1$, 1.5, 2.0 at different Prandtl numbers. The streamline representing the closed near wake is shown by a thick line.

number are found to be about 2.5% and 0.76%, respectively for both the conditions. Therefore, the grid size of 323×300 having 100 cells on each side of the cylinder has been used here.

Based on our previous study [25] and that of others [24,30], the upstream distance of 8.5 is used in this work. However, the additional computations have also been carried to explore the influence of the upstream distance for $X_u/b = 10.5$ (331×300) and for $X_u/b = 6.5$ (315×300) for the lowest Reynolds number, $Re = 1$ and the lowest Prandtl number, $Pr = 1$ at $n = 1.5$ and $X_d/b = 16.5$. The percentage changes in the values of the average Nusselt number for $X_u/b = 6.5$ and 8.5 are only 0.97% and 0.25% with respect to the value of the average Nusselt number for $X_u/b = 10.5$ for both the temperature boundary conditions. Therefore, the upstream distance of 8.5 is being used in this study.

Based on our previous study and that of others [19,24,30], the downstream distance of the cylinder from the exit plane is used as $X_d/b = 16.5$.

4. Results and discussion

In our recent study [19], we have established that the fluid flow will be steady and symmetric up to $Re = 45$ for $0.5 \leqslant n \leqslant 2.0$ for three values of the blockage ratios, i.e., $\beta = 1/8, 1/6$ and $1/4$ by carrying out the full domain ($-L_2/2b \leqslant y \leqslant L_2/2b$) calculations. Therefore, the numerical computations have been carried out for the symmetric top half of the channel ($0 \leqslant y \leqslant L_2/2b$) over the ranges as $1 \leqslant Re \leqslant 45$, $1 \leqslant n \leqslant 2.0$ and for $1 \leqslant Pr \leqslant 100$ such that the maximum value of Peclet number, Pe is 4000. The role of the two classical thermal boundary conditions, i.e., CWT and UHF has also been examined for the above range of conditions.

4.1. Validation of results

The validity of the power-law fluid flow results for the drag coefficient for $\beta = 1/8$ has been demonstrated in [19]. However, the present numerical solution procedure has also been benchmarked in number of studies in both confined and unconfined domains as reported elsewhere [12,20,22,23,25]. For the problem under consideration, a typical comparison of the normalized average Nusselt number (Nu/Nu_N) at various values of the Reynolds number and Prandtl number at $n = 1.4$ is presented in Table 1. The small discrepancy between the present results and that of Gupta et al. [2] must be due to the differences inherent in the two numerics [31]. Gupta et al. [2] have used FDM on a uni-

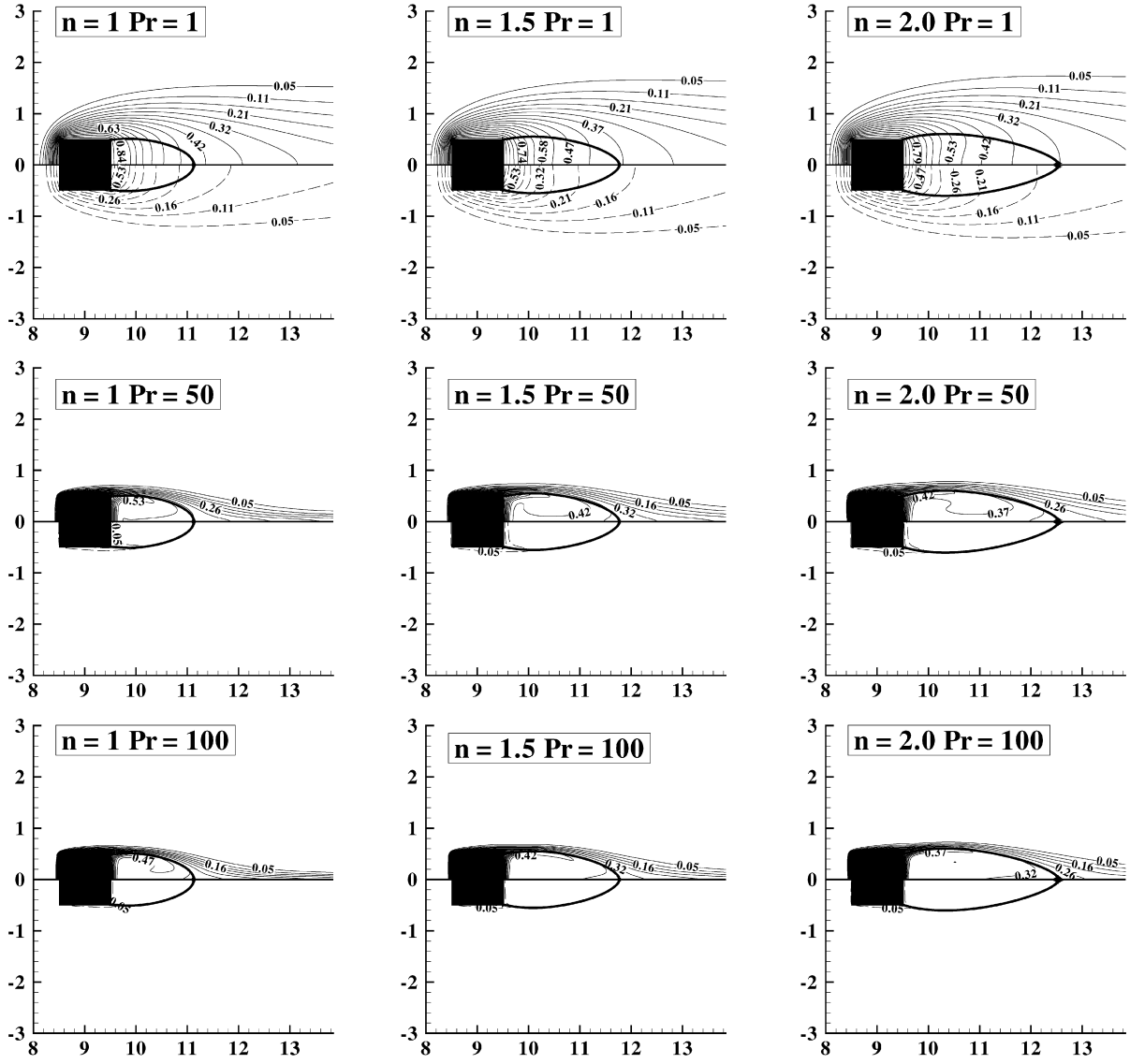

Fig. 5. Isotherms (upper and lower halves present the results for CWT and UHF cases, respectively) for $Re = 30$ and for $n = 1$, 1.5, 2.0 at different Prandtl numbers. The streamline representing the closed near wake is shown by a thick line.

Table 1
Comparison of the normalized average Nusselt number (Nu/Nu_N) with Gupta et al. [2].

Source	$Re = 5$ $Pr = 1$	$Re = 5$ $Pr = 10$	$Re = 40$ $Pr = 1$	$Re = 40$ $Pr = 10$
	$n = 1.4$			
	CWT			
Present	0.952	0.92	0.92	0.91
Gupta et al. [2]	0.964	0.94	0.95	0.94
	UHF			
Present	0.942	0.92	0.917	0.918
Gupta et al. [2]	0.958	0.94	0.944	0.945

form staggered grid arrangement (grid size = 190 × 120) without any clustering of grid points around the cylinder as well as near the channel walls. They also used a slightly shorter flow domain ($X_u/b = 6$ and $X_d/b = 12$) as opposed to the flow domain used in the present study ($X_u/b = 8.5$ and $X_d/b = 16.5$). Furthermore, Gupta et al. [2] have used only 10 cells on each side of the square obstacle as opposed to 100 cells here. The present study covers wider ranges of values of the Reynolds number ($Re = 1$, 2 and 5–45 in the steps of 5), Prandtl number ($Pr = 1$, 10, 50 and 100) and the power-law index ($n = 1$, 1.2, 1.4, 1.5, 1.6, 1.8 and 2) than that in their study. Since the flow structures, drag coefficients, etc. have been discussed in [19], therefore, in the following sections isotherm patterns, local and average Nusselt numbers, etc. have been investigated.

4.2. Isotherm patterns

Representative isotherm profiles around the square cylinder at different values of the Reynolds number, Prandtl number and power-law index have been shown in Figs. 3–6. As the fluid flow across the square object is steady and symmetric up to $Re = 45$ for $n \leqslant 2.0$ [19], the isotherm plots for the constant temperature condition are shown in the upper half of the figures while the lower half displays the corresponding results for the uniform heat flux boundary condition. Figs. 3–6 also include the closed near-wake streamline, as shown by a thick line, for $Re = 1$ at $n = 2.0$ as the flow separation has been found for the range of power-law index 1.6–2.0 at $Re = 1$ [19]. Likewise, closed near-wake streamline has also been presented for $Re = 15$, 30 and 45 at different values of the power-law index. The maximum crowding of the temper-

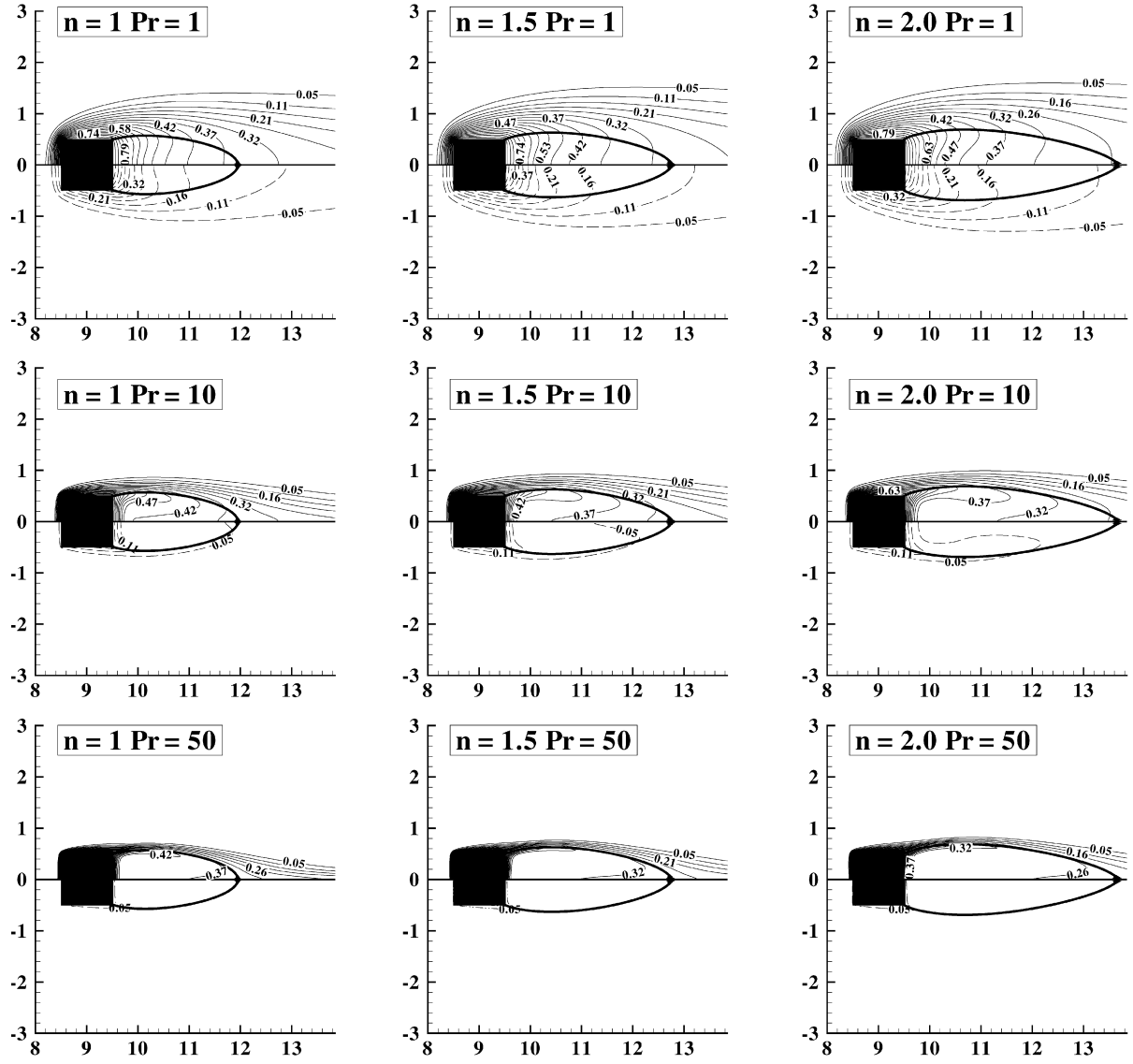

Fig. 6. Isotherms (upper and lower halves present the results for CWT and UHF cases, respectively) for $Re = 45$ and for $n = 1$, 1.5, 2.0 at different Prandtl numbers. The streamline representing the closed near wake is shown by a thick line.

ature contours can be seen at the front surface of the cylinder for both the constant temperature and the uniform heat flux boundary conditions thereby resulting in the highest Nusselt number as compared to the other surfaces of the cylinder. With the gradual increase in the value of the Reynolds number and Prandtl number irrespective of the value of the power-law index, the crowding of the temperature contours near the rear surface of the cylinder increases. Regardless of the type of temperature boundary condition, this is due to the thinning of the thermal boundary layer with the increase in the value of the Prandtl number. Decaying of temperature fields can be seen with the increase in the Prandtl number for the fixed value of the power-law index and the Reynolds number.

4.3. Local Nusselt number

In order to handle the singularity at the corners of the square obstacle, special attention was paid to the role of the grid size on the value of the local Nusselt number at each corner of the square cylinder. For this, various grid sizes have been tested as discussed in the grid resolution study and found that the grid with 100 cells on the one side of the cylinder is sufficiently fine to obtain results that are essentially grid independent [22,23].

4.3.1. Influence of constant temperature condition on local Nusselt number

The variation of the local Nusselt number for CWT condition for the symmetric top half of the channel along the cylinder front, top and rear surfaces for $Re = 1$, 15, 30 and 45 at different values of Prandtl numbers ($Pr = 1$, 10, 50 and 100) and power-law index ($n = 1$, 1.5 and 2.0) is shown in Figs. 7 (a–d). It is clear from the figure that the value of the local Nusselt number along each surface of the obstacle increases with the increasing Reynolds number and/or increasing Prandtl number for a fixed value of the power-law index. Also, it is interesting to see here that each corner of the square object shows a high value of the local Nusselt number due to the large temperature gradient normal to the surface of the obstacle. However, as the value of the power-law index increases, the local Nusselt number decreases for a fixed Reynolds and Prandtl number. Fig. 7 shows that the local Nusselt number increases towards the top corner on the front surface of the square cylinder as there is a maximum crowding of isotherms at this surface. Also, with an increase in the power-law index, there is a minimum in the local Nusselt number on this surface for a fixed value of the Reynolds number, especially at high Prandtl and Reynolds numbers. On the top surface of the cylinder, a minimum

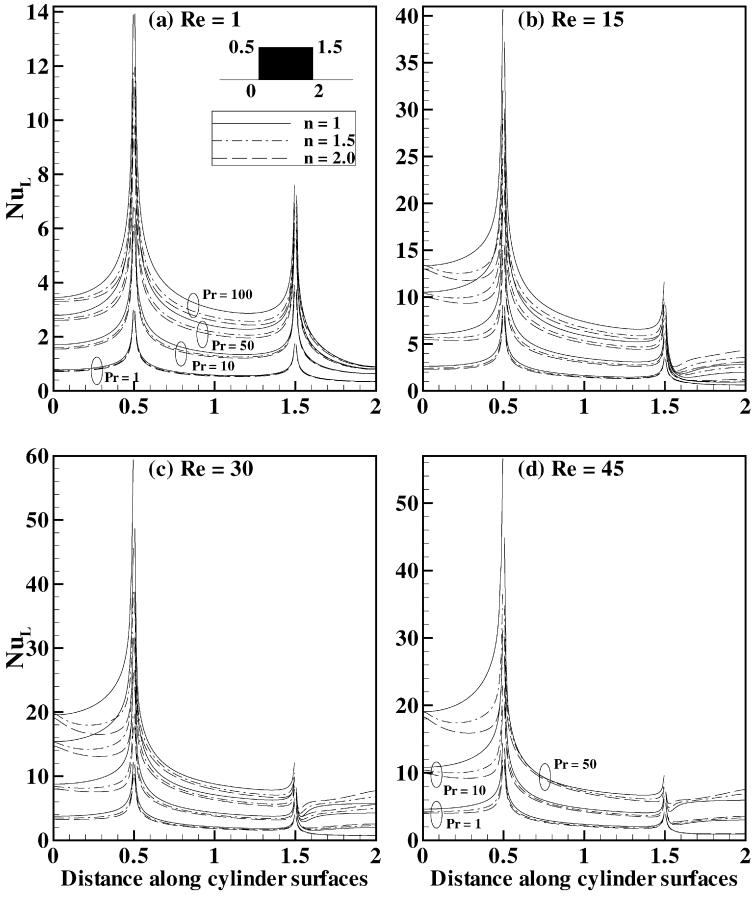

Fig. 7. Local Nusselt number variation along the cylinder surfaces from the front stagnation point to the rear stagnation point for $Re = 1$, 15, 30 and 45 ($n = 1$, 1.5, 2.0) at different Prandtl numbers for CWT case.

in the value of the local Nusselt number exists due to the turning of the isotherms near the trailing edge of the cylinder. On the rear surface of the cylinder, there is a local minimum for $Re = 1$ for different values of power-law index and Prandtl number as isotherms approach the axis of the symmetry (Fig. 7a); however, for $Re = 15$, 30, 45 for $Pr > 1$, the local minimum can be seen near the rear corner of the obstacle for the fixed values of power-law index and Reynolds number (Figs. 7 (b–d)). The values of Nusselt numbers for dilatant fluids at the rear surface of the square obstacle shows higher values than those for Newtonian fluids due to the increase in the wake region with increasing values of the Reynolds number and the power-law index for a fixed value of the Prandtl number; however, the complex (mixed) dependence has also been observed for $Re = 30$ ($Pr = 100$) and $Re = 45$ ($Pr = 50$) (Figs. 7 (c–d)).

4.3.2. Influence of uniform heat flux condition on local Nusselt number

For this condition, the representative variation of the local Nusselt number for the top half of the square cylinder along the cylinder surfaces for $Re = 1$, 15, 30 and 45 at different values of power-law index and Prandtl numbers is shown in Figs. 8 (a–d). These plots reveal qualitatively similar features as seen above for the constant temperature boundary condition case. Broadly speaking, the variation of the local Nusselt number around the cylinder for the constant heat flux condition is found to be more pronounced than that of the constant temperature condition for the range of physical parameters considered here (Fig. 8).

4.4. Average Nusselt number

As the heat transfer area is the same for each surface of the square obstacle, the overall average Nusselt number is simply the mean of the surface average values of the Nusselt number corresponding to the four surface of the cylinder.

4.4.1. Influence of constant temperature condition on average Nusselt number

Figs. 9 (a–d) show the variation of the overall average Nusselt number with Reynolds number at different values of power-law index ($n = 1$, 1.2, 1.4, 1.5, 1.6, 1.8 and 2.0) and Prandtl number ($Pr = 1$, 10, 50 and 100) for this case. The average Nusselt number increases with an increase in Reynolds number and/or Prandtl number for a fixed value of power-law index. With the increase in the value of the power-law index, the overall average Nusselt number decreases for a fixed value of the Reynolds number and the Prandtl number.

The present results have also been presented in terms of the Colburn heat transfer factor (j_h) to show the functional dependency of the flow and heat transfer parameters on this factor [22,23]. Figs. 10 (a–d) show the variation of the j_h factor with Reynolds number at different values of power-law index and Prandtl number. The j_h factor varies approximately linearly with Reynolds number at different values of the Prandtl number and the power-law index on a logarithmic scale. The following simple correlation can be used to evaluate the average Nusselt number for the range of conditions as $Re = 1$–45, $n = 1$–2.0 and $Pr = 1$–100.

$$j_h = 0.7155 Re^{-0.6136} n^{-0.20} \tag{5}$$

Eq. (5) has an average deviation of about 3.5% as compared to the computed results for 301 numerical data points. The maximum deviations are about 9.5% for $2 < Re \leqslant 45$, 14.5% for $Re = 2$ and 12.0% for $Re = 1$.

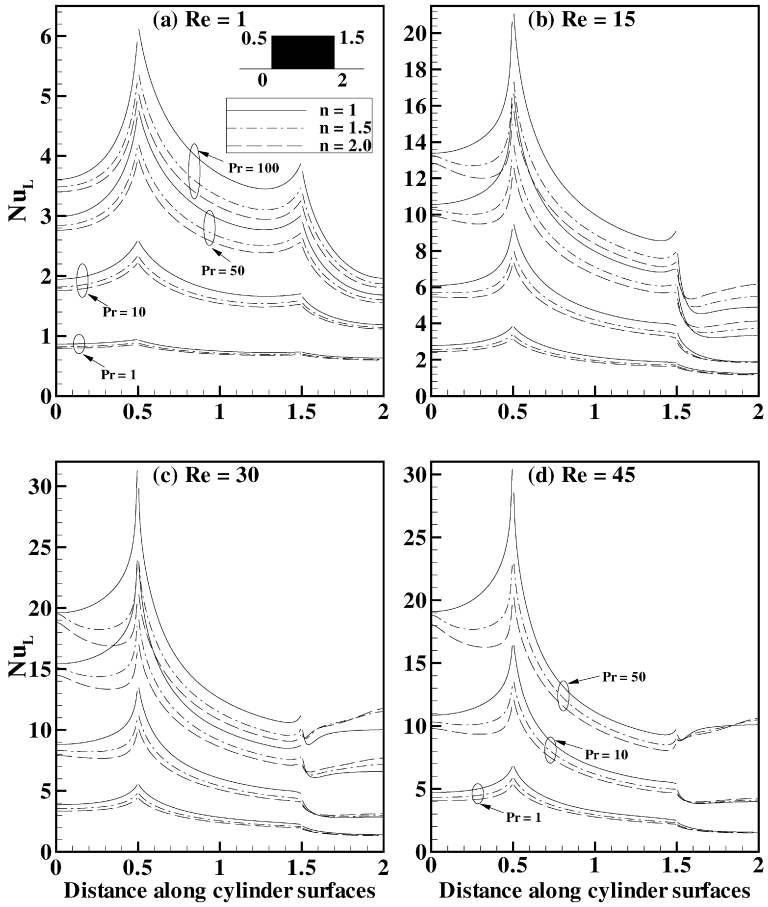

Fig. 8. Local Nusselt number variation along the cylinder surfaces from the front stagnation point to the rear stagnation point for $Re = 1$, 15, 30 and 45 ($n = 1$, 1.5, 2.0) at different Prandtl numbers for UHF case.

4.4.2. Influence of uniform heat flux condition on average Nusselt number

Here the variation of the overall average Nusselt number with the Reynolds number at different values of the power-law index and the Prandtl number is presented in Figs. 11 (a–d). It can be seen that the average Nusselt number changes in the similar fashion as observed for the case of constant temperature condition. However, the average Nusselt number always found to be higher for the constant heat flux condition than that of the constant temperature condition for dilatant fluids ($n \leqslant 2.0$) for $1 \leqslant Re \leqslant 45$ and $1 \leqslant Pr \leqslant 100$. For instance, the maximum difference ($[Nu(CHF) - Nu(CWT)]/Nu(CHF) \times 100$) in the value of the heat transfer coefficient for these two boundary conditions is of the order of 18% for $Pe = 3500$ ($Re = 35$, $Pr = 100$) and for $n = 1.2$. Figs. 10 (e–h) show the variation of j_h-factor as a function of Reynolds number and power-law index for different values of Prandtl number ($Pr = 1$, 10, 50 and $Pr = 100$). Similar dependence of j_h-factor can also be seen here as that for the constant temperature condition. In this case, the following expression can be used to calculate the average Nusselt number for the range of conditions covered in this work.

$$j_h = 0.7579 Re^{-0.5929} n^{-0.20} \tag{6}$$

This equation has an average deviation of about 3.5% as compared to the computed results for 301 numerical data points. The maximum deviations are about 8.0% for $2 < Re \leqslant 45$, 11.0% for $Re = 1$ and 2.

Eqs. (5) and (6) reduced to identical correlations for the value of the power-law index of unity (Newtonian) for CWT and UHF thermal boundary conditions as reported in our previous study [20].

Furthermore, it is observed that the ratio of the average Nusselt number for the confined case to that of the average Nusselt number for the unconfined case [23] increases up to $Re = 2$ and decreases for $2 < Re \leqslant 45$ for $Pr = 1$ for a fixed value of the power-law index for both CWT and UHF conditions. This ratio decreases monotonically with increasing Reynolds number for $Pr = 10$, 50 and 100 for CWT condition; however, for the UHF condition, the ratio decreases with increasing Reynolds number for $Pr = 10$ and has a complex (mixed) behavior for $Pr = 50$ and 100 due to the higher values of the average Nusselt number for the unbounded case than that of the average Nusselt number for the bounded case. The maximum relative changes in the values of the ratio are 16.5%, 11.5%, 5.9% and 3.5% for $Re = 1, 2, 5$ and 10–45, respectively for different values of the power-law index and the Prandtl number for the uniform wall temperature condition. The corresponding changes in the values of the ratio are 15.5%, 11.0%, 5.6% and 4.0% for $Re = 1$, 2, 5 and 10–45, respectively for different values of the power-law index and the Prandtl number for the uniform heat flux condition. This ratio decreases with increasing value of the power-law index for a fixed value of the Reynolds number for both the temperature boundary conditions; however, the ratio has a complex behavior for $Pr = 50$ and 100 for the UHF condition.

5. Conclusions

In this study, the effects of Reynolds number and Prandtl number on the heat transfer characteristics of dilatant fluids ($n \leqslant 2.0$) across the square cylinder confined in a channel has been investigated for the varying range of Reynolds number ($1 \leqslant Re \leqslant 45$) and Prandtl number ($1 \leqslant Pr \leqslant 100$) for the constant temperature

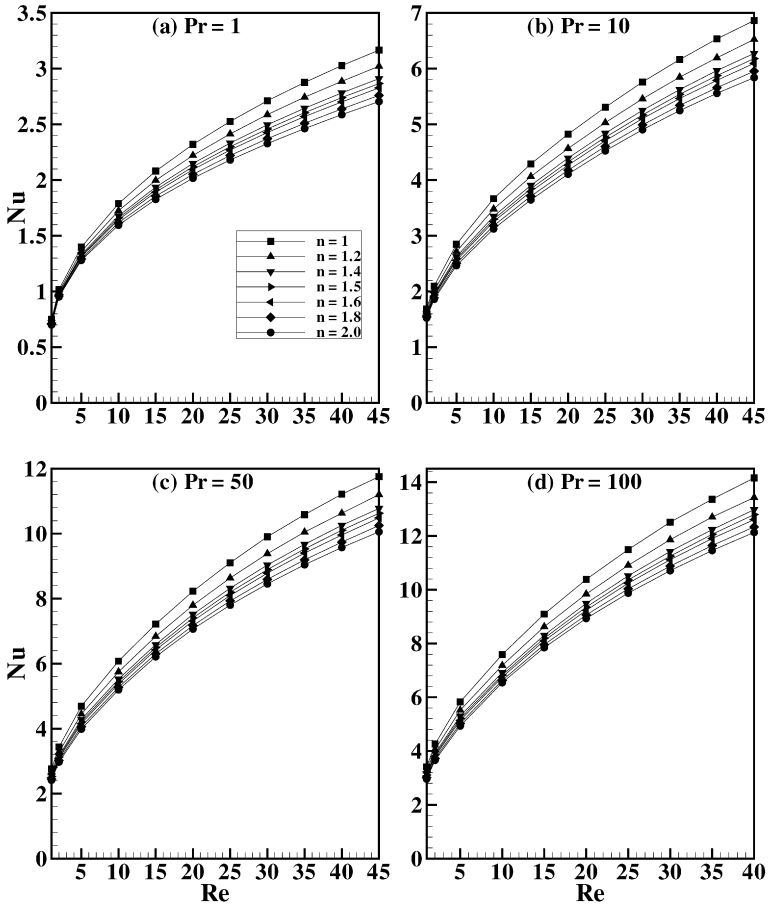

Fig. 9. Variation of the average Nusselt number for the cylinder as a function of Reynolds number for $Pr = 1$, 10, 50 and 100 at different power-law index for CWT case.

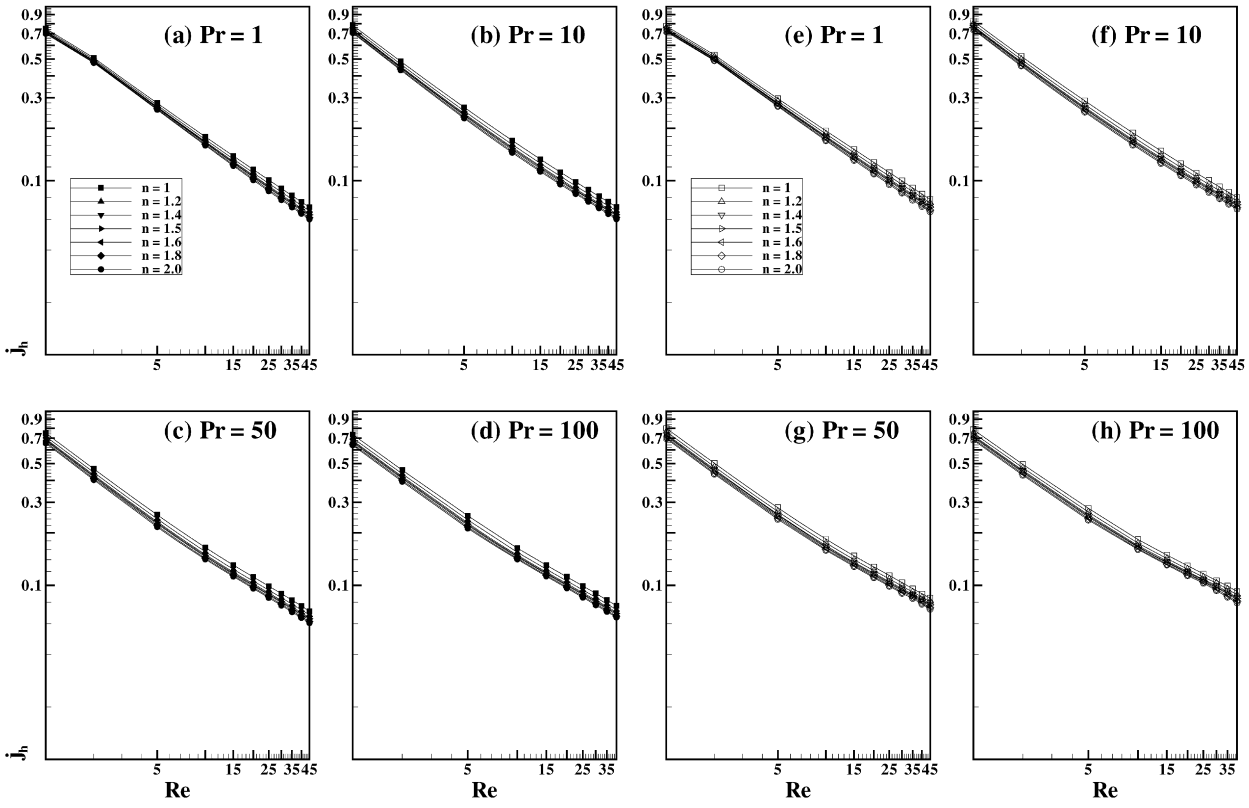

Fig. 10. The Colburn j_h factor as a function of Reynolds number for $Pr = 1$, 10, 50 and 100 at different power-law index for CWT (a–d) and UHF (e–h) cases.

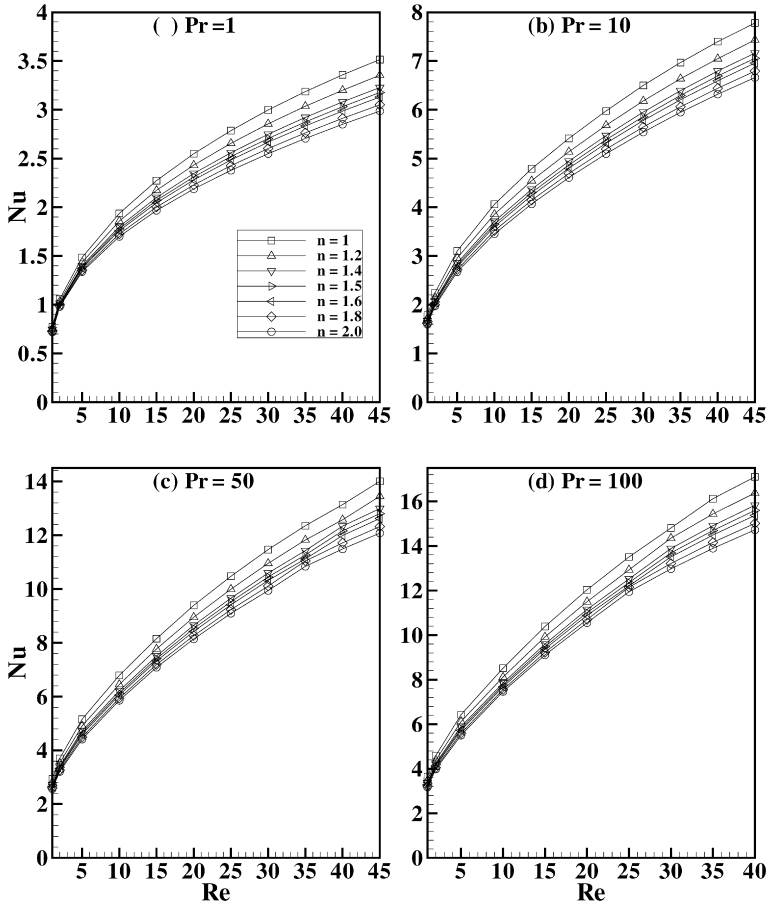

Fig. 11. Variation of the average Nusselt number for the cylinder as a function of Reynolds number for $Pr = 1$, 10, 50 and 100 at different power-law index for UHF case.

and uniform heat flux conditions. The local Nusselt number at each corner of the square cylinder increases with an increase in the Reynolds number and/or Prandtl number irrespective of the value of the power-law index. The average Nusselt number increases monotonically with an increase in the Reynolds number and/or the Prandtl number. Broadly, the average Nusselt number is always higher for the case of uniform heat flux boundary condition than that for the constant temperature condition for the same values of the Reynolds and Prandtl numbers and the power law index. Finally, simple heat transfer correlations have been obtained for both the thermal boundary conditions.

References

[1] S.J.D. D'Alessio, J.P. Pascal, Steady flow of a power-law fluid past a cylinder, Acta Mechanica 117 (1996) 87–100.
[2] A.K. Gupta, A. Sharma, R.P. Chhabra, V. Eswaran, Two-dimensional steady flow of a power law fluid past a square cylinder in a plane channel: momentum and heat transfer characteristics, Ind. Eng. Chem. Res. 42 (2003) 5674–5686.
[3] B. Paliwal, A. Sharma, R.P. Chhabra, V. Eswaran, Power law fluid flow past a square cylinder: momentum and heat transfer characteristics, Chem. Eng. Sci. 58 (2003) 5315–5329.
[4] S.J.D. D'Alessio, L.A. Finlay, Power-law flow past a cylinder at large distances, Ind. Eng. Chem. Res. 43 (2004) 8407–8410.
[5] R.P. Chhabra, A.A. Soares, J.M. Ferreira, Steady non-Newtonian flow past a circular cylinder: a numerical study, Acta Mechanica 172 (2004) 1–16.
[6] J.M. Ferreira, R.P. Chhabra, Analytical study of drag and mass transfer in creeping power-law flow across tube banks, Ind. Eng. Chem. Res. 43 (2004) 3439–3450.
[7] A.A. Soares, J.M. Ferreira, R.P. Chhabra, Flow and forced convection heat transfer in cross-flow of non-Newtonian fluids over a circular cylinder, Ind. Eng. Chem. Res. 44 (2005) 5815–5827.
[8] S. Nitin, R.P. Chhabra, Non-isothermal flow of a power-law fluid past a rectangular obstacle (of aspect ratio 1×2) in a channel: drag and heat transfer, Int. J. Eng. Sci. 43 (2005) 707–720.
[9] W.A. Khan, J.R. Culham, M.M. Yovanovich, Fluid flow and heat transfer in power-law fluids across circular cylinder-analytical study, J. Heat Transfer 128 (2006) 870–878.
[10] P. Sivakumar, R.P. Bharti, R.P. Chhabra, Effect of power-law index on critical parameters for power-law flow across an unconfined circular cylinder, Chem. Eng. Sci. 61 (2006) 6035–6046.
[11] R.P. Bharti, R.P. Chhabra, V. Eswaran, Steady flow of power-law fluids across a circular cylinder, Can. J. Chem. Eng. 84 (2006) 406–421.
[12] A.K. Dhiman, R.P. Chhabra, V. Eswaran, Steady flow of power-law fluids across a square cylinder, Chem. Eng. Res. Des. 84 (2006) 300–310.
[13] R.P. Bharti, R.P. Chhabra, V. Eswaran, Two-dimensional steady Poiseuille flow of power-law fluids across a circular cylinder in a plane confined channel: wall effects and drag coefficients, Ind. Eng. Chem. Res. 46 (2007) 3820–3840.
[14] R.P. Bharti, R.P. Chhabra, V. Eswaran, Steady forced convection heat transfer from a heated circular cylinder to power-law fluids, Int. J. Heat Mass Transfer 50 (2007) 977–990.
[15] R.P. Bharti, R.P. Chhabra, V. Eswaran, Effect of blockage on heat transfer from a cylinder to power-law liquids, Chem. Eng. Sci. 62 (2007) 4729–4741.
[16] R.P. Chhabra, Bubbles, Drops and Particles in Non-Newtonian Fluids, 2nd edition, CRC Press, Boca Raton, FL, 2006.
[17] R.P. Chhabra, J.F. Richardson, Non-Newtonian Flow in the Process Industries, Butterworth-Heinemann, Oxford, 1999.
[18] R.P. Chhabra, Hydrodynamics of non-spherical particles in non-Newtonian fluids, in: N.P. Cheremisinoff, P.N. Cheremisinoff (Eds.), Handbook of Applied Polymer Processing Technology, Marcel Dekker, N.Y., 1996 (Chapter 1).
[19] A.K. Dhiman, R.P. Chhabra, V. Eswaran, Steady flow across a confined square cylinder: effects of power-law index and blockage ratio, J. Non-Newtonian Fluid Mech. 148 (2008) 141–150.
[20] A.K. Dhiman, R.P. Chhabra, V. Eswaran, Flow and heat transfer across a confined square cylinder in the steady flow regime: effect of Peclet number, Int. J. Heat Mass Transfer 48 (2005) 4598–4614.
[21] A.K. Dhiman, R.P. Chhabra, V. Eswaran, Effect of Peclet number on the heat transfer across a square cylinder in the steady confined channel flow regime, in: Proc. 18th National and 7th ISHMT–ASME Heat and Mass Transfer Conf., Indian Institute of Technology Guwahati, India, 2006.
[22] A.K. Dhiman, R.P. Chhabra, A. Sharma, V. Eswaran, Effects of Reynolds and Prandtl numbers on heat transfer across a square cylinder in the steady flow regime, Numerical Heat Transfer A 49 (2006) 717–731.

[23] A.K. Dhiman, R.P. Chhabra, V. Eswaran, Heat transfer to power-law fluids from a heated square cylinder, Numerical Heat Transfer A 52 (2007) 185–201.
[24] A. Sharma, V. Eswaran, Heat and fluid flow across a square cylinder in the two-dimensional laminar flow regime, Num. Heat Transfer A 45 (2004) 247–269.
[25] A.K. Dhiman, N. Anjaiah, R.P. Chhabra, V. Eswaran, Mixed convection from a heated square cylinder to Newtonian and power-law fluids, Trans. ASME J. Fluids Eng. 129 (2007) 506–513.
[26] A.K. Dhiman, R.P. Chhabra, V. Eswaran, Steady mixed convection across a confined square cylinder, Int. Comm. Heat Mass Transfer 35 (2008) 47–55.
[27] J.F. Thompson, Z.U.A. Warsi, C.W. Mastin, Numerical Grid Generation: Foundations and Applications, Elsevier Science, New York, 1985, pp. 305–310.
[28] K.A. Hoffmann, Computational Fluid Dynamics for Engineers, Engineering Education System, Austin, TX, 1989.
[29] V. Eswaran, S. Prakash, A finite volume method for Navier–Stokes equations, in: Proc. Third Asian CFD Conference, Bangalore, India, vol. 1, 1998, pp. 127–136.
[30] A. Sharma, V. Eswaran, A finite volume method, in: K. Muralidhar, T. Sundararajan (Eds.), Computational Fluid Flow and Heat Transfer, Narosa Publishing House, New Delhi, 2003, pp. 445–482.
[31] P.J. Roache, Verification and Validation in Computational Science and Engineering, Hermosa, Albuquerque, NM, 1998.